Extracting effective normal modes from equilibrium dynamics at finite temperature

M. Martinez, M.-P. Gaigeot, D. Borgis, and R. Vuilleumier

Citation: The Journal of Chemical Physics **125**, 144106 (2006); doi: 10.1063/1.2346678
View online: https://doi.org/10.1063/1.2346678
View Table of Contents: http://aip.scitation.org/toc/jcp/125/14
Published by the American Institute of Physics

Extracting effective normal modes from equilibrium dynamics at finite temperature

M. Martinez
Laboratoire de Physique Théorique de la Matière Condensée, Université Pierre et Marie Curie, Paris 6, UMR 7600, Tour 24-25, 2ème Étage, 4 Place Jussieu, F-75005 Paris, France

M.-P. Gaigeot
Laboratoire de Physique Théorique de la Matière Condensée, Université Pierre et Marie Curie, Paris 6, UMR 7600, Tour 24-25, 2ème Étage, 4 Place Jussieu, F-75005 Paris, France and Laboratoire Analyse et Modélisation pour la Biologie et l'Environnement, Université d'Evry val d'Essonne, UMR 8587, Rue Père A. Jarland, F-91025 Evry, France

D. Borgis
Laboratoire Analyse et Modélisation pour la Biologie et l'Environnement, Université d'Evry val d'Essonne, UMR 8587, Rue Père A. Jarland, F-91025 Evry, France

R. Vuilleumier[a)]
Laboratoire de Physique Théorique de la Matière Condensée, Université Pierre et Marie Curie, Paris 6, UMR 7600, Tour 24-25, 2ème Étage, 4 Place Jussieu, F-75005 Paris, France

(Received 12 June 2006; accepted 8 August 2006; published online 11 October 2006)

A general method for obtaining effective normal modes of a molecular system from molecular dynamics simulations is presented. The method is based on a localization criterion for the Fourier transformed velocity time-correlation functions of the effective modes. For a given choice of the localization function used, the method becomes equivalent to the principal mode analysis (PMA) based on covariance matrix diagonalization. On the other hand, a proper choice of the localization function leads to a novel method with a strong analogy with the usual normal mode analysis of equilibrium structures, where the Hessian system at the minimum energy structure is replaced by the thermal averaged Hessian, although the Hessian itself is never actually calculated. This method does not introduce any extra numerical cost during the simulation and bears the same simplicity as PMA itself. It can thus be readily applied to *ab initio* molecular dynamics simulations. Three such examples are provided here. First we recover effective normal modes of an isolated formaldehyde molecule computed at 20 K in very good agreement with the results of a normal mode analysis performed at its equilibrium structure. We then illustrate the applicability of the method for liquid phase studies. The effective normal modes of a water molecule in liquid water and of a uracil molecule in aqueous solution can be extracted from *ab initio* molecular dynamics simulations of these two systems at 300 K. © *2006 American Institute of Physics*. [DOI: 10.1063/1.2346678]

I. INTRODUCTION

Vibrational spectroscopy (infrared and Raman or in a certain way inelastic neutron scattering) can provide valuable information about the chemical state of a molecule and the structure and dynamics of its environment. Assignment of vibrational modes is an important step in the interpretation of these data as fingerprints of conformations and solvation. Modeling and numerical simulations can be very helpful in this respect. However, this necessitates accurate intra- and intermolecular potentials, able to describe both the typical intramolecular motions of the molecule under study and also the induced shifts due to conformational changes or due to the interaction with the environment. Such potential should then incorporate correctly anharmonic terms and polarization effects, in particular at finite temperature.

Lately, density functional theory (DFT) based molecular dynamics (MD) was proven successful for the computation of vibrational spectra. In these simulations the forces acting on the atoms are obtained at each time step of the simulation by an electronic structure calculation in the DFT framework.[1] This thus combines accurate description of forces in many environments and situations while providing a description of the structure and dynamics of a system in its fluctuating environment at finite temperature. Since the pioneering work of Silvestrelli *et al.* for the computation of the infrared spectrum of liquid water,[2] DFT-based MD has been applied successfully to the calculation of IR spectra of pure liquids,[3,4] of solvated ions in organic solvents,[5] or of small biological molecules in aqueous solution,[6–10] or Raman spectra in condensed phase.[11,12]

Direct comparison of the infrared spectra from DFT-based MD with experiment was made possible by the definition of polarization for periodic systems by Resta, using the concept of Berry phase.[13] The infrared spectrum is then

[a)]Electronic mail: vuilleum@lptl.jussieu.fr

expressed through the linear response theory as the Fourier transform of the dipole, or current, autocorrelation function,[14]

$$I(\omega) \propto \int dt \langle \mathbf{M}(0)\mathbf{M}(t)\rangle e^{i\omega t} \tag{1}$$

$$\propto \int dt \langle \mathbf{j}(0)\mathbf{j}(t)\rangle e^{i\omega t}, \tag{2}$$

where $\mathbf{M}$ is the total dipole and $\mathbf{j}(t)=d\mathbf{M}(t)/dt$ the total current in the simulated sample. This, however, does not provide a simple way of assigning vibrational bands to molecular motions, which is probably the primary goal of the modeling of vibrational spectra. Based on the expression of the infrared signal as an autocorrelation function of the current, tentative assignments can be done through the Fourier transform of the atomic velocity autocorrelation functions (FTVCFs) or power spectra,

$$P_I(\omega) = \int dt \langle \mathbf{v}_I(0)\mathbf{v}_I(t)\rangle e^{i\omega t} \tag{3}$$

(for an atom labeled I). These power spectra then give information on the typical frequencies of the motion of individual atoms and, at a given frequency, the different atoms participating in a given vibrational mode can be identified.[8] Further information on symmetries can help to determine the vibrational motion under scrutiny, but no quantitative data is easily attainable this way for systems of more than three to four atoms.

In the present work we describe a systematic method for decomposing vibrational spectra as an approximate sum of effective normal mode contributions. We will define these effective normal modes from the data of the FTVCF, so that they will be extracted directly from the MD trajectory. The effective normal modes will be linear combinations of atomic displacements constructed such that the corresponding power spectra will be as localized as possible in frequency. There is no loss of information from this transformation which is just a change of coordinates.

Other methods have been proposed in the literature for assigning or approximating vibrational spectra such as spectral analysis,[15–19] instantaneous normal mode analysis and its variants,[20–25] and principal mode analysis[26–29] (PMA) and essential dynamics,[30–32] both based on the diagonalization of covariance matrices. Instantaneous normal mode analysis, however, requires many calculation of the Hessian system which can become quickly prohibitive for DFT-based MD simulation. Due to its simplicity PMA has lately attracted attention.[27,28,33–35]

Here we will show that our new general definition for effective normal modes, based on a localization principle in frequency space, not only leads at zero temperature to the usual normal mode analysis but is also consistent with the PMA approach. Moreover, it provides another route to extract an effective Hessian and effective normal modes at finite temperature.

Three examples of application of this new scheme will then be presented, using DFT-based MD trajectories. We have determined as a first test the effective normal modes of a formaldehyde molecule at $T=20$ K in the gas phase. Then we have focused on the vibrational spectroscopy of one water molecule in liquid water. Finally, results for the larger uracil molecule in aqueous solution will be presented.

In Sec. II, we will develop the theory of effective normal modes from a localization principle of their power spectra in frequency space. After discussing how this can lead to a vibrational spectra decomposition and band assignment, we will discuss the solution of the localization problem. We will then show that it leads exactly to a normal mode analysis at $T=0$ while providing a natural extension for $T\neq 0$. The link with PMA will then be highlighted by deriving this theory from the proposed localization prescription. We will finally relate these approaches to force-fitting procedures.

In Sec. III we will then present the extraction of effective normal modes from DFT-based MD simulations of the three systems above mentioned. We will then conclude in Sec. IV.

II. THEORY

A. Fourier transformed velocity time-correlation functions

We consider a molecular system consisting of N atoms, treated classically, and we denote by $\mathbf{x}(t)=(x_1(t),\ldots,x_{3N}(t))$ the vector made from the set of the $3N$ coordinates of the system at time t, and by $\mathbf{p}(t)=(p_1(t),\ldots,p_{3N}(t))$ the vector of momenta in the *laboratory* frame. The dynamical properties of the system will be studied through time-correlation functions $\langle A(0)B(t)\rangle$, where A and B are microscopic observables depending on the instantaneous positions $(\mathbf{x},\mathbf{p})$ of the system in phase space and $\langle\ \rangle$ denotes an equilibrium average (either in the canonical or microcanonical ensembles).

From the matrix of the velocity time-correlation functions, $\langle \dot{x}_i(0)\dot{x}_j(t)\rangle$, including both self- and cross terms, we introduce the matrix $\mathbf{P}^{\dot{x}}(\omega)\equiv P_{ij}^{\dot{x}}(\omega)$ of FTVCF,

$$P_{ij}^{\dot{x}}(\omega) = \int_{-\infty}^{+\infty} \langle \dot{x}_i(0)\dot{x}_j(t)\rangle e^{i\omega t} dt. \tag{4}$$

In the case $i=j$, $P_{ii}^{\dot{x}}(\omega)$ is usually called the power spectrum of the coordinate x_i. The matrix $\mathbf{P}^{\dot{x}}(\omega)$ of FTVCF satisfies

$$P_{ij}^{\dot{x}}(\omega) = P_{ji}^{\dot{x}*}(\omega) = P_{ij}^{\dot{x}*}(-\omega). \tag{5}$$

This last property is still true when the time-correlation functions are estimated from a finite time molecular dynamics simulation. If, furthermore, we consider exact ensemble averages for a time-reversible (infinitely long) dynamics then $\mathbf{P}^{\dot{x}}(\omega)$ is a real symmetric matrix; the following discussion is, however, not limited to this case.

For any observable A which is a linear combination of the coordinates, $A(t)=\Sigma_i a_i x_i(t)=\mathbf{a}^T\mathbf{x}(t)$, with $\mathbf{a}=(a_1,\ldots,a_{3N})$, the power spectrum of A can simply be written as

$$P_A(\omega) = \int_{-\infty}^{+\infty} \langle \dot{a}(0)\dot{a}(t)\rangle e^{i\omega t} dt = \mathbf{a}^T\mathbf{P}^{\dot{x}}(\omega)\mathbf{a}. \tag{6}$$

This matrix is, in general, highly nondiagonal and the full matrix, not just the power spectra of the Cartesian coordinates, is thus needed in order to calculate the FTVCF of any

quantity $A(t)$ due to correlation between the atomic velocities arising from the coupled motion of different atoms.

An interesting property of the FTVCF matrix appears for a system in thermal equilibrium either in the microcanonical or in the canonical ensemble. In that case, the velocities of Cartesian coordinates are decorrelated on average for $i \neq j$, and their variance is given by the temperature and the mass m_i of the atom associated with the Cartesian coordinate x_i,[36]

$$\langle \dot{x}_i \dot{x}_j \rangle = \frac{k_B T \delta_{ij}}{m_i}, \tag{7}$$

where k_B is the Boltzmann constant and δ_{ij} the Kroenecker symbol. The temperature T is either the thermostat temperature in the canonical ensemble or defined through the thermodynamical relation $1/T = \partial S/\partial E$ in the microcanonical ensemble.[36] From the properties of the inverse Fourier transform, this is equivalent to

$$\frac{1}{2\pi}\int_{-\infty}^{+\infty} d\omega P_{ij}^{\dot{x}}(\omega) = \frac{k_B T \delta_{ij}}{m_i}. \tag{8}$$

The nondiagonal terms of the FTVCF matrix have thus an integral over frequencies equal to zero. For an operator A as defined above, this leads to

$$\langle \dot{A}\dot{A} \rangle = k_B T \sum_i \frac{a_i^2}{m_i}, \tag{9}$$

and $\langle \dot{A}\dot{A} \rangle$ can be written as a sum of terms associated with each coordinate independently.

B. Localization of FTVCF

Our goal here is to define vibrational modes from which we can describe the trajectory of the whole system, and of any observable A, in a simpler manner than using the Cartesian coordinates themselves. This is done by decomposing the system trajectory into $3N$ components $\mathbf{q}(t) \equiv (q_1(t), \ldots, q_{3N}(t))$.[37] Using Einstein's notation,

$$x_i(t) = Z_{ik} q_k(t), \tag{10a}$$

$$\dot{x}_i(t) = Z_{ik} \dot{q}_k(t), \tag{10b}$$

where the matrix $\mathbf{Z} = (Z_{ij})$ is inversible and, at this stage, unknown. For these modes, we also define a FTVCF matrix as

$$P_{kl}^{\dot{q}}(\omega) = \int_{-\infty}^{+\infty} \langle \dot{q}_k(0) \dot{q}_l(t) \rangle e^{i\omega t} dt. \tag{11}$$

These modes should be as independent as possible, and the first requirement for the vibrational modes q_k, as suggested by previous authors,[34,35] is that the property (7) is fulfilled,

$$\langle \dot{q}_k \dot{q}_l \rangle = \frac{1}{2\pi}\int_{-\infty}^{+\infty} d\omega P_{kl}^{\dot{q}}(\omega) = k_B T \delta_{kl}, \tag{12}$$

where, by choice here, we impose that all mode velocities have the same variance, $k_B T$. The property of decorrelation at equilibrium for the velocities $\dot{x}_i$ is thus enforced on the vibrational modes by definition. From (7), it can be shown that this implies that the modes q_k are obtained from *any* unitary transformation of the mass weighted coordinates, $u_i = \sqrt{m_i} x_i$, which is usual in a normal mode analysis of minimum energy structures.[37] This can be viewed as a justification of the present choice of Eq. (7) although this last property, that the modes q_k are unitary transformations of the mass weighted coordinates, now appears as a consequence of the required decorrelation of the velocities $\dot{q}_k$ at time $t=0$. This is, however, not sufficient to uniquely determine effective normal modes.

For a nonequivocal definition of normal modes, we thus propose to further require that the power spectra of the vibrational modes q_k be as localized as possible in frequency. This can be achieved, for example, by looking for the modes which minimize, under the constraint given by Eq. (12), the quantity,

$$\Omega^{(n)} = \sum_k \left(\frac{\beta}{2\pi}\int_{-\infty}^{+\infty} d\omega |\omega|^{2n} P_{kk}^{\dot{q}}(\omega) - \left(\frac{\beta}{2\pi}\int_{-\infty}^{+\infty} d\omega |\omega|^{n} P_{kk}^{\dot{q}}(\omega) \right)^2 \right), \tag{13}$$

where $n \neq 0$ is a free integer and $\beta = 1/k_B T$.

By application of the Wiener-Khintchine theorem, the power spectra $P_{kk}^{\dot{q}}(\omega)$ are necessarily real and positive, and by means of the normalization enforced in Eq. (12), $\Omega^{(n)}$ can be interpreted as

$$\Omega^{(n)} = \sum_k (\langle \omega^{2n} \rangle_k - \langle \omega^n \rangle_k^2), \tag{14}$$

where $\langle f(\omega) \rangle_k$ is the average of a function $f(\omega)$ over all positive frequencies weighted by the power spectrum of mode k.

We propose that this minimization criterion is a generalization of the normal modes to anharmonic systems at temperature T and can serve to extract vibrational modes from MD simulations to interpret calculated vibrational spectra. A natural choice for n in Eq. (13) would be $n=1$, for which $\langle \omega^2 \rangle_k - \langle \omega \rangle_k^2$ is then the standard deviation of the power spectrum of mode k. The above criterion can, however, be extended to any even function of ω. The natural choice of $n=1$ turns out to have no obvious physical interpretation, whereas we will show later that the choice of $n=-2$ leads to the principal mode analysis while the choice of $n=2$ will have a very strong analogy with the normal mode analysis (NMA) of minimum structures, generalized to anharmonic systems in equilibrium at finite temperature T.

The power spectra of the effective normal modes being maximally localized, we can hope that those will be made essentially of single peaks centered around well defined frequencies. The effective normal modes could then be used by simple inspection to interpret vibrational spectra of the system, in terms of molecular vibrations.

Furthermore, as another consequence of the Wiener-Khintchine theorem, since for all observable A defined as linear combination of the coordinates, the associated power spectrum $P_A(\omega)$ is positive, the matrices $\mathbf{P}^{\dot{x}}(\omega)$ and $\mathbf{P}^{\dot{q}}(\omega)$ are

positive definite for all ω. This implies a Cauchy-Schwartz relationship for the off-diagonal terms of $\mathbf{P}^{\dot{q}}(\omega)$,

$$|P^{\dot{q}}_{kl}(\omega)| \leqslant \sqrt{(P^{\dot{q}}_{kk}(\omega)P^{\dot{q}}_{ll}(\omega))}. \tag{15}$$

Thus if the power spectra of two modes k and l are well localized around different frequencies, the overlap between these power spectra, and thus the right-hand side of Eq. (15), will be small for all ω. In this sense, the modes k and l will be nearly decorrelated.

For an observable A defined as a linear combination of the coordinates, which we will rewrite now as $A=\Sigma_k a'_k q_k$, the power spectrum of A can then be approximated by

$$P_A(\omega) = \sum_{kl} a'_k a'_l P^{\dot{q}}_{kl}(\omega) \approx \sum_k a'^2_k P^{\dot{q}}_{kk}(\omega). \tag{16}$$

As we shall show later, both the result of the constraint (12) and the minimization criterion imply that the integral and the nth moment of the spectrum $P_A(\omega)$, approximated as a sum of effective normal mode contributions [right-hand side of Eq. (16)], are both exact.

More generally, for an observable $A(\mathbf{x})$ which can depend nonlinearly on the atomic positions, we have

$$\dot{A}(t) = \sum_i \frac{\partial A}{\partial x_i}\dot{x}_i = \sum_k \frac{\partial A}{\partial q_k}\dot{q}_k, \tag{17}$$

so that the power spectrum of A is written as

$$\begin{aligned} P_A(\omega) &= \int_{-\infty}^{+\infty} \langle \dot{A}(0)\dot{A}(t)\rangle e^{i\omega t} dt \\ &= \sum_{kl} \int_{-\infty}^{+\infty} \left\langle \left(\frac{\partial A}{\partial q_k}\dot{q}_k\right)(0)\left(\frac{\partial A}{\partial q_l}\dot{q}_l\right)(t)\right\rangle e^{i\omega t} dt. \end{aligned} \tag{18}$$

From the near decorrelation of the velocities $\dot{q}_k$, the power spectrum of A could again be approximated by a sum of single mode quantities,

$$P_A(\omega) \approx \sum_k \int_{-\infty}^{+\infty} \left\langle \left(\frac{\partial A}{\partial q_k}\dot{q}_k\right)(0)\left(\frac{\partial A}{\partial q_k}\dot{q}_k\right)(t)\right\rangle e^{i\omega t} dt. \tag{19}$$

C. Effective normal modes from finite time simulations

A problem arises when we are estimating effective normal modes from finite time molecular dynamics simulations. In that case, the equipartition [Eq. (7)] may not be exactly satisfied if sampling is not sufficient. This is particularly pertinent for *ab initio* MD simulations for which until now only short simulation times are achievable. In that case, we face the choice, when constructing approximate effective normal modes for the simulated system, between restricting the modes to unitary transformations of mass weighted coordinates or exactly satisfying Eq. (12). We have found that solving the minimization problem under the constraint (12) gives better decomposition of vibrational spectra, since the integral and nth moment of simulated vibrational spectra are preserved after decomposition in effective modes [Eq. (16)]. This decomposition of vibrational spectra is our primary goal, and quantities such as typical mode frequencies are readily obtained with this choice, without need of further renormalizations as in previous works. In the following, we will also show that this choice does guarantee that harmonic systems will generate modes that are collinear to the exact normal modes, even with bad statistics.

The distance between the estimated modes and unitary transformations of mass weighted coordinates is then a measure of violation of equipartition, and better modes, closer to unitary transforms of mass weighted coordinates, can be obtained with better statistics. This distance could also be used to improve simulated vibrational spectra by enforcing equipartition *a posteriori* in the spirit of Ref. 34. We will give hints on such approaches in the following, but we have not tried to apply them numerically.

D. Solution of the minimization problem

We now solve the minimization problem and show that the effective normal modes can be constructed explicitly without having to use a minimization procedure. We first rewrite Eq. (10) in a matrix form,

$$\mathbf{x} = \mathbf{Z}\mathbf{q}, \tag{20a}$$

$$\dot{\mathbf{x}} = \mathbf{Z}\dot{\mathbf{q}}, \tag{20b}$$

where the matrix $\mathbf{Z}=(Z_{ik})$ is the unknown transformation matrix between the modes q_k and the Cartesian coordinates x_i. We can further write the mode velocities $\dot{\mathbf{q}}$ as linear combinations of the momenta $\mathbf{p}$ rather than velocities $\dot{\mathbf{x}}$,

$$\dot{\mathbf{q}} = \mathbf{Y}^T\mathbf{p}, \tag{21}$$

where we have used a contravariant form with respect to the definition of $\dot{\mathbf{q}}$ from velocities. The matrices $\mathbf{Y}$ and $\mathbf{Z}$ are related by

$$\mathbf{M}\mathbf{Y} = \mathbf{Z}^{T^{-1}}, \tag{22}$$

where $\mathbf{M}$ is a $3N\times 3N$ (N being the number of atoms) diagonal matrix composed of the atomic masses,

$$\mathbf{M} = \begin{pmatrix} m_1 & & & & & & & & \\ & m_1 & & & & & & & \\ & & m_1 & & & & & & \\ & & & \ddots & & & & & \\ & & & & \ddots & & & & \\ & & & & & m_N & & & \\ & & & & & & m_N & & \\ & & & & & & & m_N & \end{pmatrix}. \tag{23}$$

Then from

$$\langle \dot{q}_k(0)\dot{q}_l(t)\rangle = Y_{ik}\langle p_i(0)p_j(t)\rangle Y_{jl}, \tag{24}$$

the matrices of FTVCF for $\mathbf{p}$ and $\dot{\mathbf{q}}$ are related by

$$\mathbf{P}^{\dot{q}}(\omega) = \mathbf{Y}^T\mathbf{P}^p(\omega)\mathbf{Y}. \tag{25}$$

The constraint (12) is now written as

$$\frac{\beta}{2\pi}\int_{-\infty}^{+\infty} d\omega \mathbf{P}^{\dot{q}}(\omega) = \mathbf{Y}^T \mathbf{K}_p^{(0)} \mathbf{Y} = \mathbf{I}_{3N}. \tag{26}$$

In a matrix form, $\mathbf{I}_{3N}$ is the identity matrix at $3N$ dimension and the matrix $\mathbf{K}_p^{(0)}$ is given by

$$\mathbf{K}_p^{(0)} = \frac{\beta}{2\pi}\int_{-\infty}^{+\infty} d\omega \mathbf{P}^{p}(\omega). \tag{27}$$

For equilibrium averages at temperature T, we have [see Eq. (8)]

$$(K_p^{(0)})_{ij} = m_i \delta_{ij} \tag{28a}$$

or

$$\mathbf{K}_p^{(0)} = \mathbf{M}. \tag{28b}$$

The matrix $\mathbf{K}_p^{(0)}$ is in that case the diagonal matrix of atomic masses and Eq. (26) can then be written at equilibrium

$$\mathbf{Y}^T \mathbf{M} \mathbf{Y} = \mathbf{I}_{3N}. \tag{29}$$

The quantity $\Omega^{(n)}$ to be minimized under constraint (26) can be written as a function of the unknown transformation matrix $\mathbf{Y}$,

$$\Omega^{(n)} = \left[\mathrm{Tr}(\mathbf{Y}^T \mathbf{K}_p^{(2n)} \mathbf{Y}) - \sum_k (\mathbf{Y}^T \mathbf{K}_p^{(n)} \mathbf{Y})_{kk}^2 \right], \tag{30}$$

where we defined for any integer m, $\mathbf{K}_p^{(m)}$ similar to $\mathbf{K}_p^{(0)}$,

$$\mathbf{K}_p^{(m)} = \frac{\beta}{2\pi}\int_{-\infty}^{+\infty} d\omega |\omega|^m \mathbf{P}^{p}(\omega). \tag{31}$$

From the properties (5) of the FTVCF, the matrices $\mathbf{K}_p^{(m)}$ are real symmetric for all integer m.

We also remark that

$$\mathrm{Tr}[\mathbf{Y}^T \mathbf{K}_p^{(2n)} \mathbf{Y}] = \mathrm{Tr}[\mathbf{K}_p^{(2n)} \mathbf{Y} \mathbf{Y}^T] \tag{32a}$$

$$= \mathrm{Tr}[\mathbf{K}_p^{(2n)} \mathbf{K}_p^{(0)^{-1}}] \tag{32b}$$

is independent of $\mathbf{Y}$. The last equality arises from Eq. (26) and the fact that $\mathbf{Y}$ is inversible.

Minimizing $\Omega^{(n)}$ then amounts to maximizing

$$\Omega'^{(n)} = \sum_k (\mathbf{Y}^T \mathbf{K}_p^{(n)} \mathbf{Y})_{kk}^2, \tag{33}$$

under the constraint of Eq. (26).

We show in Appendix A that doing so is equivalent to solving the generalized eigenvalue problem

$$K_{pij}^{(n)} Y_{jk}^0 = \lambda_k^{(n)} K_{pij}^{(0)} Y_{jk}^0, \tag{34a}$$

$$\mathbf{K}_p^{(n)} \mathbf{Y}^0 = \mathbf{K}_p^{(0)} \mathbf{Y}^0 \Lambda, \tag{34b}$$

for $\mathbf{Y}^0$ under constraint (26). We now have a way to define effective modes that are localized in frequency space by solving this generalized eigenvalue problem.

The matrix $\mathbf{Z}^0$ which defines the coordinate transformation between Cartesian coordinates and effective normal modes can subsequently be obtained from $\mathbf{Y}^0$ through Eq. (22). We can also derive $\mathbf{Z}^0$ from a generalized eigenvalue problem: from Eqs. (22) and (34), $\mathbf{Z}^{0^{-1}}$ is found to be the solution of the generalized eigenvalue problem

$$\mathbf{Z}^{0^{-1}} \mathbf{K}_x^{(n)} = \Lambda^{(n)} \mathbf{Z}^{0^{-1}} \mathbf{K}_x^{(0)} \tag{35}$$

under the constraint

$$\mathbf{Z}^{0^{-1}} \mathbf{K}_x^{(0)} \mathbf{Z}^{0^{-1^T}} = \mathbf{I}_{3N}, \tag{36}$$

where we define $\mathbf{K}_x^{(m)}$ as $\mathbf{K}_p^{(m)}$

$$\mathbf{K}_x^{(m)} = \frac{\beta}{2\pi}\int_{-\infty}^{+\infty} d\omega |\omega|^m \mathbf{P}^{\dot{x}}(\omega). \tag{37}$$

However, in the case where the system is in equilibrium at temperature T, constraint (26) becomes constraint (29) which can be compared to Eq. (22) and leads simply to $\mathbf{Z}^0 = \mathbf{Y}^0$ in that case.

Construction of the effective normal modes through the solution of the localization problem is then reduced to simply solving a linear problem, which can be done by standard linear algebra routines. In the next sections, we will focus on two cases, $n=2$ and $n=-2$, where it will be shown that the FTVCF matrices do not need to be computed to construct the matrices $\mathbf{K}_p^{(2)}$ and $\mathbf{K}_x^{(-2)}$: these are covariance matrices of accelerations and positions, respectively.

A few remarks can be made at this stage. First, note that all $\mathbf{K}_x^{(m)}$ and $\mathbf{K}_p^{(m)}$ are proportional to $\beta = 1/k_B T$ so that if we would consider β as a free normalization parameter for constructing effective modes from a simulated dynamics, we find that a solution $\mathbf{Y}^0$ is to be simply renormalized for another choice β': $\mathbf{Y}^0 \rightarrow \beta/\beta' \mathbf{Y}^0$. This does not change qualitatively the effective normal modes and leaves the eigenvalues $\lambda_k^{(n)}$ invariant. Second, constructing analogous $\mathbf{K}$ matrices for the modes q,

$$\mathbf{K}_q^{(m)} = \frac{\beta}{2\pi}\int_{-\infty}^{+\infty} d\omega |\omega|^m \mathbf{P}^{\dot{q}}(\omega), \tag{38}$$

where $\mathbf{K}_q^{(m)}$ is related to $\mathbf{K}_p^{(m)}$ by

$$\mathbf{K}_q^{(m)} = \mathbf{Y}^T \mathbf{K}_p^{(m)} \mathbf{Y}, \tag{39}$$

the generalized eigenvalue problem [Eq. (34)] can then be rewritten as

$$\mathbf{K}_q^{(n)} = \mathbf{K}_q^{(0)} \Lambda, \tag{40}$$

and for a particular mode k we have $(\mathbf{K}_q^{(n)})_{kk} = \lambda_k^{(n)} (\mathbf{K}_q^{(0)})_{kk}$, that is,

$$\lambda_k^{(n)} = \frac{\int_{-\infty}^{+\infty} d\omega |\omega|^n P_{kk}^{\dot{q}}(\omega)}{\int_{-\infty}^{+\infty} d\omega P_{kk}^{\dot{q}}(\omega)}. \tag{41}$$

The eigenvalues $\lambda_k^{(n)}$ are then the averages $\langle \omega^n \rangle_k$ of ω^n over the power spectra of modes q_k. Furthermore, using constraint (26), we find $\mathbf{K}_q^{(0)} = \mathbf{I}_{3N}$, implying $\mathbf{K}_q^{(n)} = \Lambda^{(n)}$. These two matrices are then diagonal, and this leads to the above mentioned fact that upon approximating the power spectrum $P_A(\omega)$ of an observable A as a sum of independent power spectra of the effective normal modes [Eq. (16)], the integral and the nth moment of $P_A(\omega)$ are exact.

As a final remark, we note that it can be proven that the above minimization principle and associated eigenvalue for-

mulation can be extended to inhomogeneous broadening situations in which the Hamiltonian system is time dependent although on a long time scale.

E. $n=2$: Analogy with normal mode analysis

Let's consider the case $n=2$ for a system at equilibrium in the microcanonical or canonical ensembles, T being the system temperature. In that case we can explicitly construct the matrix $\mathbf{K}_p^{(2)}$, and the generalized eigenvalue problem (34) then constitutes a natural extension of the normal mode analysis of minimum energy structure to finite temperature and anharmonic system while being exactly equivalent to it for harmonic systems at all temperatures.

Elements of $\mathbf{K}_p^{(2)}$ are

$$(\mathbf{K}_p^{(2)})_{ij} = \frac{\beta}{2\pi}\int_{-\infty}^{+\infty} d\omega\omega^2 P_{ij}^p(\omega) = \frac{\beta}{2\pi}\int_{-\infty}^{+\infty} d\omega\omega^2 \mathrm{TF}[\langle p_i(0)p_j(t)\rangle](\omega). \tag{42}$$

Using properties of the Fourier transform, we immediately find

$$(\mathbf{K}_p^{(2)})_{ij} = -\frac{\beta}{2\pi}\int_{-\infty}^{+\infty} d\omega \mathrm{TF}\left[\frac{d^2}{dt^2}\langle p_i(0)p_j(t)\rangle\right](\omega) \tag{43}$$

and

$$(\mathbf{K}_p^{(2)})_{ij} = -\beta \left.\frac{d^2}{dt^2}\langle p_i(0)p_j(t)\rangle\right|_{t=0}. \tag{44}$$

Using the stationarity of the correlation functions, we find

$$(\mathbf{K}_p^{(2)})_{ij} = \beta\langle F_i(0)F_j(t)\rangle|_{t=0} = \beta\langle F_i F_j\rangle, \tag{45}$$

where F_i is the ith component of the force acting on the system. This allows construction of the matrix $\mathbf{K}_p^{(2)}$ without the need to calculate the full spectra $P_{ij}^p(\omega)$. With similar arguments we can easily show that

$$(\mathbf{K}_p^{(0)})_{ij} = \beta\langle p_i(0)p_j(t)\rangle|_{t=0} = \beta\langle p_i p_j\rangle. \tag{46}$$

In the case $n=2$ the generalized eigenvalue problem to be solved is then

$$\langle F_i F_j\rangle Y_{jk} = \langle\omega^2\rangle_k \langle p_i p_j\rangle Y_{jk}. \tag{47}$$

This equation is generally applicable to finite time simulations. Further simplification can be made, however, for exact thermodynamics equilibrium statistics, either in the microcanonical or canonical ensemble.

Indeed, an interesting property of equilibrium situations in both ensembles is the relation between force fluctuations and the Hessian system, related to what is now known as conformational temperature.[36,38] Applied to the case at hand, we have

$$k_B T = \frac{\langle(\partial V/\partial x_i)(\partial V/\partial x_j)\rangle}{\langle \partial^2 V/\partial x_i \partial x_j\rangle}, \tag{48}$$

where V is the system potential energy and $\partial^2 V/\partial x_i \partial x_j$ the Hessian system.

Elements of $\mathbf{K}_p^{(2)}$ are thus

$$(\mathbf{K}_p^{(2)})_{ij} = \left\langle \frac{\partial^2 V}{\partial x_i \partial x_j}\right\rangle, \tag{49}$$

so that the generalized eigenvalue problem to be solved in order to construct localized modes is

$$\left\langle \frac{\partial^2 V}{\partial x_i \partial x_j}\right\rangle Z_{jk} = \langle\omega^2\rangle_k m_i Z_{ik}, \tag{50}$$

with the constraint $Z_{ik}m_i Z_{il} = \delta_{kl}$ [we have used $\mathbf{Y}=\mathbf{Z}$ and $\mathbf{K}_p^{(0)} = (\langle p_i p_j\rangle) = \mathbf{M}$, as noted precedently]. This is exactly the equation for normal modes,[37] which are unitary transforms of the mass weighted coordinates, where the Hessian at the minimum energy structure is to be replaced by the average Hessian at finite temperature T, showing the strong analogy between the two approaches. Note that it is not necessary to construct the Hessian along the dynamics, which would be prohibitively expensive for *ab initio* MD, as the average Hessian is constructed from the force fluctuations at equilibrium.

F. $n=-2$: Comparison to PMA

For the choice of $n=-2$ it is also possible to explicitly construct the matrices for the generalized eigenvalue problem (34). Using here Eq. (35) for $\mathbf{Z}^{-1}$ instead of the equation for $\mathbf{Y}$, we have to inspect the matrices $\mathbf{K}_x^{(0)}$ and $\mathbf{K}_x^{(-2)}$, respectively. Elements of the matrix $\mathbf{K}_x^{(0)}$ are

$$(\mathbf{K}_x^{(0)})_{ij} = \frac{\beta}{2\pi}\int_{-\infty}^{+\infty} d\omega P_{ij}^{\dot{x}}(\omega) = \frac{\beta}{2\pi}\int_{-\infty}^{+\infty} d\omega \mathrm{TF}[\langle \dot{x}_i(0)\dot{x}_j(t)\rangle](\omega), \tag{51}$$

which simply leads to

$$(\mathbf{K}_x^{(0)})_{ij} = \beta\langle \dot{x}_i \dot{x}_j\rangle \tag{52}$$

and $\mathbf{K}_x^{(0)} = \mathbf{M}^{-1}$ at equilibrium. Similarly, for $\mathbf{K}_x^{(-2)}$ we have

$$(\mathbf{K}_x^{(-2)})_{ij} = \frac{\beta}{2\pi}\mathcal{P}\int_{-\infty}^{+\infty} d\omega\omega^{-2} P_{ij}^{\dot{x}}(\omega) = \frac{\beta}{2\pi}\mathcal{P}\int_{-\infty}^{+\infty} d\omega\omega^{-2} \mathrm{TF}[\langle \dot{x}_i(0)\dot{x}_j(t)\rangle](\omega), \tag{53}$$

where for $n<0$ we use the principal part $\mathcal{P}$ for defining the nth moment of the FTVCF (see Appendix B for details). For $\mathbf{K}_x^{(-2)}$ to be finite, it is necessary that $\mathrm{TF}[\langle \dot{x}_i(0)\dot{x}_j(t)\rangle](\omega) \to 0$ as $\omega \to 0$, that is,

$$\int_{-\infty}^{+\infty} \langle \dot{x}_i(0)\dot{x}_j(t)\rangle dt = 0; \tag{54}$$

there should be no diffusive modes in principle in the system under consideration when employing $n=-2$ for constructing localized modes. From

$$\frac{d^2}{dt^2}\langle \delta x_i(0)\,\delta x_j(t)\rangle = -\langle \dot{x}_i(0)\dot{x}_j(t)\rangle, \tag{55}$$

with $\delta x_i = x_i - \langle x_i\rangle$ the atomic displacements with respect to the average atomic position, we have

$$\omega^2 \mathrm{TF}[\langle \delta x_i(0)\, \delta x_j(t)\rangle](\omega) = \mathrm{TF}[\langle \dot{x}_i(0)\dot{x}_j(t)\rangle](\omega) \tag{56}$$

or, for $\omega \neq 0$,

$$\mathrm{TF}[\langle \delta x_i(0)\, \delta x_j(t)\rangle](\omega) = \frac{1}{\omega^2}\mathrm{TF}[\langle \dot{x}_i(0)\dot{x}_j(t)\rangle](\omega). \tag{57}$$

After integration over all ω, we can explicitly express (see Appendix B) $\mathbf{K}_x^{(-2)}$ as

$$(\mathbf{K}_x^{(-2)})_{ij} = \frac{\langle \delta x_i \delta x_j\rangle}{k_B T}. \tag{58}$$

$\mathbf{K}_x^{(-2)}$ is then the covariance matrix of the atomic displacements and the generalized eigenvalue problem to be solved can be rewritten as

$$(\langle \delta\mathbf{x}\,\delta\mathbf{x}^T\rangle^{-1})_{ij} Z_{jk} = \frac{1}{\langle \omega^{-2}\rangle_k}(\langle \dot{\mathbf{x}}\dot{\mathbf{x}}^T\rangle^{-1})_{ij} Z_{jk} \tag{59}$$

or, for fully equilibrated trajectories,

$$(\langle \delta\mathbf{x}\,\delta\mathbf{x}^T\rangle^{-1})_{ij} Z_{jk} = \frac{\beta}{\langle \omega^{-2}\rangle_k} m_i Z_{ik}. \tag{60}$$

This is exactly the PMA method, in which the covariance matrix in mass weighted coordinates is diagonalized,[27,28] but here it has been derived from the localization principle and the choice of $n=-2$. It also generates the normal modes of a harmonic system at all temperatures.

The PMA procedure has been extended previously to take into account deficiencies of the statistics when averages are obtained from short time simulations.[33,34] This connects to the present approach when using Eq. (59). In particular, we will show in the following that for a strictly harmonic system, the present method leads to modes strictly collinear with the true normal modes, even when only poor equipartition is achieved. This will be based on a different point of view for the construction of effective normal modes: we will show that for the special cases $n=-2$ and $n=2$ the localization principle is equivalent to a force-fitting prescription.

G. Effective normal modes as a force-fitting procedure

1. n=−2 case

Equation (59) can be straightforwardly rewritten

$$(\langle \dot{\mathbf{x}}\dot{\mathbf{x}}^T\rangle)_{li}(\langle \delta\mathbf{x}\,\delta\mathbf{x}^T\rangle^{-1})_{ij} Z_{jk} = \frac{1}{\langle \omega^{-2}\rangle_k} Z_{lk}. \tag{61}$$

From $\langle \dot{x}_l \dot{x}_i\rangle = -\langle \ddot{x}_l \delta x_i\rangle = -(1/m_l)\langle F_l \delta x_i\rangle$, this leads to

$$-(\langle \mathbf{F}\,\delta\mathbf{x}^T\rangle)_{li}(\langle \delta\mathbf{x}\,\delta\mathbf{x}^T\rangle^{-1})_{ij} Z_{jk} = \frac{1}{\langle \omega^{-2}\rangle_k} m_l Z_{lk}. \tag{62}$$

In Appendix C we show that the matrix $k_{lj} = -(\langle \mathbf{F}\,\delta\mathbf{x}^T\rangle)_{li}(\langle \delta\mathbf{x}\,\delta\mathbf{x}^T\rangle^{-1})_{ij}$ is the best harmonic approximation or best fit of the true forces F_i by a linear combination of the atomic displacements

$$F_i \approx -k_{i1}\delta x_1 - \cdots - k_{i,3N}\delta x_{3N} = -k_{ij}\delta x_j. \tag{63}$$

k_{ij} is the solution of a least-squares fit, minimizing the error,

$$\chi = \sum_i \langle (F_i + k_{i1}\delta x_1 + \cdots + k_{i,3N}\delta x_{3N})^2\rangle. \tag{64}$$

The PMA equation is thus equivalent to

$$k_{lj} Z_{jk} = \frac{1}{\langle \omega^{-2}\rangle_k} m_l Z_{lk}. \tag{65}$$

This is strictly a normal mode analysis equation where the best harmonic potential in a least-squares sense is considered.

For equilibrium situations at temperature T, we have $\langle F_l \delta x_i\rangle = k_B T \delta_{li}$ such that k_{lj}, giving the "best" harmonic forces, is simply proportional to the inverse of the covariance matrix $\langle \delta x_i \delta x_j\rangle$.

For a harmonic system, on the other hand, even for imperfect statistics, k_{ij} is the symmetric matrix of harmonic force constants for the system. From its symmetry property and Eq. (65) it is possible to show that the matrix $\mathbf{Z}^T\mathbf{M}\mathbf{Z}$ commutes with the diagonal matrix of mode pulsations $1/(\omega^{-2})_k$. If all mode frequencies are different, the matrix $\mathbf{Z}^T\mathbf{M}\mathbf{Z}$ is then diagonal $[(1/\langle\omega^{-2}\rangle_k)(\mathbf{Z}^T\mathbf{M}\mathbf{Z})_{kl} - (\mathbf{Z}^T\mathbf{M}\mathbf{Z})_{kl}(1/\langle\omega^{-2}\rangle_l) = 0]$. It is, however, not necessarily unity as equipartition may not be satisfied in a short simulation; however, modes could be renormalized according to the diagonal elements of $\mathbf{Z}^T\mathbf{M}\mathbf{Z}$ leading to a new matrix $\mathbf{Z}$ which would be a unitary transformation of mass weighted coordinates and still satisfy Eq. (65). The modes obtained through the localization principle for the choice of $n=-2$ for a harmonic system are thus collinear to the true normal modes of the system, up to this renormalization.

If the system is anharmonic, however, and if equipartition is not verified, then the matrix k_{ij} defined above by least-squares fitting of the forces as linear combination of atomic displacements is not necessarily symmetric anymore, and the approximate effective modes are not simply related to unitary transformation of mass weighted coordinates. An approach to improve on such approximation would be to impose symmetry of the matrix k_{ij} in the least-squares procedure and renormalize the modes, as just mentioned. This could help also to correct the predicted vibrational spectra by imposing the equipartition condition.

2. n=2 case

A similar analysis can be performed when the choice of $n=2$ is made. From the same considerations as in the previous section, the elements of the matrix $\mathbf{K}_x^{(2)}$ can be shown to be equal to

$$k_B T(\mathbf{K}_x^{(2)})_{ij} = \langle \ddot{x}_i \ddot{x}_j\rangle = m_i^{-1}\langle F_i \ddot{x}_j\rangle = -m_i^{-1}\langle \dot{F}_i \dot{x}_j\rangle. \tag{66}$$

The generalized eigenvalue problem of which $\mathbf{Z}$ is a solution [Eq. (35)] is then

$$-\mathbf{Z}^{-1}\mathbf{M}^{-1}\langle\dot{\mathbf{F}}\dot{\mathbf{x}}^T\rangle = \langle\omega^2\rangle\mathbf{Z}^{-1}\langle\dot{\mathbf{x}}\dot{\mathbf{x}}^T\rangle, \tag{67a}$$

$$\mathbf{Z}^{-1}\mathbf{M}^{-1}(-\langle\dot{\mathbf{F}}\dot{\mathbf{x}}^T\rangle\langle\dot{\mathbf{x}}\dot{\mathbf{x}}^T\rangle^{-1}) = \langle\omega^2\rangle\mathbf{Z}^{-1}. \tag{67b}$$

Multiplying this equation by **MZ** on the left and **Z** on the right and introducing the matrix $k'_{ij}=(-\langle\dot{\mathbf{F}}\dot{\mathbf{x}}^T\rangle\langle\dot{\mathbf{x}}\dot{\mathbf{x}}^T\rangle^{-1})_{ij}$ we find again a normal mode analysis with the force constant matrix k'_{ij},

$$k'_{ij}Z_{jk} = M_i Z_{jk}\langle\omega^2\rangle_k. \tag{68}$$

The force constant k'_{ij} are here obtained from a fit of the time derivative of the forces as linear combination of atomic velocities,

$$\dot{F}_i \approx -k_{i1}\dot{x}_1 - \cdots - k_{i,3N}\dot{x}_{3N} = -k_{ij}\dot{x}_j, \tag{69}$$

by minimization of

$$\chi = \sum_i \langle(\dot{F}_i + k_{i1}\dot{x}_1 + \cdots + k_{i,3N}\dot{x}_{3N})^2\rangle. \tag{70}$$

The case of $n=2$ also amounts then to map the system with an adapted harmonic system. At equilibrium, the best force constants are here the average Hessian matrix (see discussion above), as could be expected.

H. Frame of reference

For a system that possesses rotational invariance, molecules in gas phase or in liquid phase, we have to face an additional problem. Upon considering the Cartesian coordinates $\{x_i\}_{i=1,\ldots,3N}$ as coordinates with respect to a fixed laboratory frame, then many out-of-diagonal terms in the matrices $\mathbf{K}_p^{(n)}$ and $\mathbf{K}_x^{(n)}$ are set to zero by symmetry and it is not guaranteed that it would be possible to construct localized modes in frequency as a linear combination of Cartesian coordinates in a fixed frame. It is convenient then to introduce a set of coordinates $z_i(t)$, $i=1,\ldots,3N$ with respect to a mobile frame bound to the molecule. The natural frame for this purpose is the Eckart frame,[39] considering the equilibrium (or eventually a mean structure) $\mathbf{r}_I^0$, $I=1,\ldots,N$ of the molecular system. The instantaneous Eckart frame is defined by the constraints

$$\sum_I m_I\mathbf{z}_I = 0, \tag{71}$$

$$\sum_I m_I\mathbf{r}_I^0 \wedge \mathbf{z}_I = 0, \tag{72}$$

which ensure that the center of mass of the system is maintained at the origin and the absence of net rotation of the system. From the $3N$ coordinates z_i, only $3N-6$ are then independent. This mobile frame minimizes the rovibrational couplings while it depends only on the system coordinates in the fixed frame (no other explicit or history dependent dependency). It is possible to show that the Eckart frame can be constructed simply through a least-squares fit of the instantaneous configuration using the equilibrium configuration, that is, minimizing

$$\sum_i m_i(r_i^0 - z_i)^2 = \sum_i m_i\xi_i^2, \tag{73}$$

where we have introduced the displacement vectors ξ_i of atoms with respect to their equilibrium position in the mobile frame.

Once we have then determined the moving Eckart frame and deduced the trajectory $\{z_i(t)\}_{i=1,\ldots,3N}$ of the atoms in this frame, we can use the preceding results for constructing localized modes from the dynamics. However, we are facing two possibilities. The method described in the previous sections is based on the use of correlation functions of atomic *velocities*, and it amounts maybe more to a decomposition of the atomic velocities [Eq. (20b)] rather than to a decomposition of the displacements [Eq. (20a)]. Should these velocities be velocities with respect to the fixed laboratory frame but expressed in a system of coordinates bound to the Eckart frame [rotations of the velocities $\dot{x}_i(t)$ from the laboratory system of coordinates to the instantaneous Eckart coordinate system] or velocities in the mobile frame [simply the vectors $\dot{z}_i(t)$]?

In the former case, when we consider velocities with respect to the laboratory frame but expressed in the system of coordinates of the Eckart frame, the $3N$ velocities are independent and are not restricted to the Eckart conditions. The $3N$ localized modes do not themselves satisfy the Eckart conditions, but we may expect from the use of the mobile system of coordinates, which should minimize rovibrational couplings, that six of the modes will be mainly rotations and translations, while $3N-6$ should be vibrational modes, approximately satisfying the Eckart conditions (by orthogonality with respect to the first six modes). It is interesting to note that formal relations for equilibrium correlation functions are still valid, in particular $\mathbf{K}_p^{(0)}=\mathbf{M}$, arising from the decoupling at equilibrium between positions (that alone determines the Eckart frame) and velocities in the laboratory frame. The link with NMA is thus strictly preserved in this approach.

In the latter case, however, six modes should have strictly zero eigenvalues while $3N-6$ should strictly satisfy the Eckart conditions. At this point the previous equations are not complete: constraint (26) is not sufficient as the matrix $\mathbf{K}_p^{(0)}$ is not positive definite anymore and the solution to the generalized eigenvalue problem (34) is not unique. We have to explicitly specify that six modes are rotation and translation and $3N-6$ are constrained to the Eckart conditions. If we rewrite the Eckart conditions for the modes $k=1,\ldots,3N-6$ in a vectorial form as

$$T_i^\alpha Z_{ik} = 0, \tag{74}$$

$$R_i^\alpha Z_{ik} = 0, \tag{75}$$

for $\alpha=x,y,z$ the principal axis of the molecule in its reference geometry, and for the translation and rotation conditions, respectively, it can be shown that those additional constraints can be incorporated directly in the generalized eigenvalue problem (34) by replacing $\mathbf{K}_p^{(0)}$ by

$$\mathbf{K}_p'^{(0)} = \mathbf{K}_p^{(0)} + \sum_{\alpha=x,y,z} T^{\alpha T} T^{\alpha} + R^{\alpha T} R^{\alpha}. \quad (76)$$

in Eqs. (26) and (34). This leads to six pure modes of translation and rotation and $3N-6$ vibrational modes strictly satisfying the Eckart conditions.

In one of the examples discussed below, for the determination of effective normal modes of one water molecule in liquid water, both approaches will be compared and they will be shown to lead to very similar results, although in the first case, information is gained about the typical frequencies and power spectra of the translations and rotations of the water molecule in its cage.

III. APPLICATIONS

A. Simulation details

In the three examples discussed in the following sections, we have generated a trajectory for each system using density functional theory (DFT) based *ab initio* molecular dynamics (MD).[1] The exchange-correlation functional used in each case was BLYP.[40,41] Electronic orbitals and the electronic density were expanded in a plane wave basis set (with a 70 Ry cutoff), and periodic boundary conditions were employed. As a consequence, atoms were pseudized and only valence electrons were taken into account. For this purpose we have used norm-conserving Martins-Troullier pseudopotentials[42] in a semilocal form.[43] Electronic degrees of freedom were propagated along the nuclei dynamics using the Car-Parrinello (CP) method;[1] all simulations were realized with the CPMD package.[44]

In each case, we have obtained effective normal modes using the effective Hessian approach, $n=2$ in the theory developed above, since we think it provides a more natural approach to vibrational analysis than PMA, $n=-2$, although its applicability has still to be demonstrated, unlike PMA. Since all trajectories are only a few picoseconds long (see below), it was important to solve the generalized eigenvalue problem described by (47) to obtain meaningful effective normal modes instead of (50) which assumes complete thermodynamics equilibrium.

B. Isolated formaldehyde molecule at 20 K

In a first example, we have looked for the effective normal modes of a formaldehyde molecule in gas phase at low temperature $T=20$ K. This system stays close to its potential energy minimum during the dynamics, and we would like to check that effective normal modes reconstructed from an *ab initio* molecular dynamics trajectory are close to the normal modes calculated from the Hessian at the optimized geometry. The formaldehyde molecule has C_{2v} symmetry with three vibrational modes of A_1 character, two of B_2 character, and one of B_1; it is of interest to see how these mode symmetries are recovered by the construction of the effective normal modes and if the mixing between modes of the same symmetry is well reproduced (particularly the mixing of C═O stretch and HCH bending).

One CP trajectory for one formaldehyde molecule in a 10 Å box was generated with a time step $\delta t=0.048$ fs and a fictitious electronic mass $\mu_e=200$ a.u. After an equilibration period, data were accumulated for 7 ps, with a sampling of the trajectory for analysis purpose (power spectra calculation) every ten steps. We have also independently optimized the geometry of the formaldehyde molecule and calculated the Hessian using linear response DFT.[11]

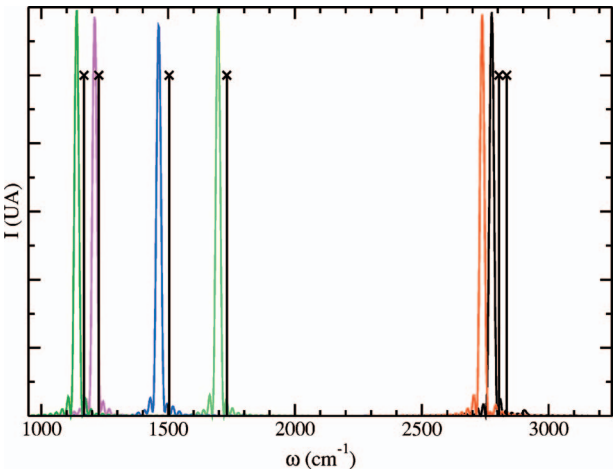

FIG. 1. (Color) Power spectra of the effective normal modes of H_2CO at $T=20$ K in the Eckart framework rotating with the molecule (color lines) and the eigenvalues of the Hessian at $T=0$ K (vertical line with a cross at the top).

The effective normal modes were extracted from the formaldehyde trajectory at $T=20$ K, in the rotating Eckart *framework*. Figure 1 shows the power spectra of the effective normal modes thus obtained. It is clear from this figure that the power spectrum of each effective normal mode forms a single peak well localized in frequency, with negligible overlap between modes. The sinc tails and the width of these peaks are due to the finite simulation length (7 ps). The peak frequencies of the effective normal modes at $T=20$ K are in good agreement with the normal mode frequencies at the equilibrium geometry (see Fig. 1) with a slight redshift which might be due to the fictitious electronic dynamics in the Car-Parrinello simulation.

Nevertheless, excellent agreement between the effective normal modes reconstructed from the 20 K dynamics and the normal modes at equilibrium is obtained (see Fig. 2). The mode characters are well recovered by the procedure of localization in frequency of the effective normal mode power spectra.

C. Water molecules in liquid water

Given this encouraging result for a gas phase molecule we have applied the effective normal mode analysis to the dynamics of a water molecule in liquid water. A short 3 ps Car-Parrinello dynamics of a system comprising 32 water molecules at $T=300$ K in a 9.86 $Å^3$ cubic box was generated with a time step $\delta t=0.12$ fs and a fictitious electron mass $\mu_e=500$ a.u. This trajectory was also sampled every ten steps. The short simulation time is compensated by averages over the 32 water molecules to get better statistics. Averaging was performed on the velocity autocorrelation functions and

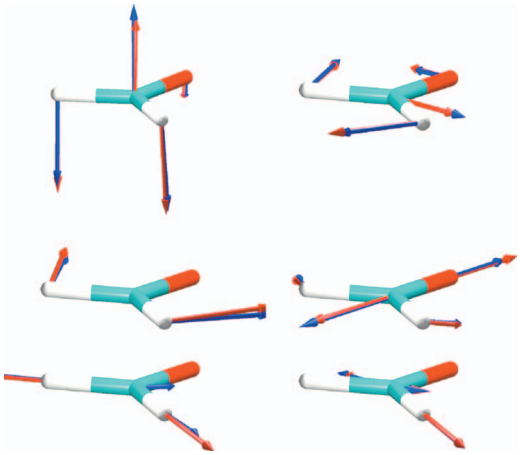

FIG. 2. (Color) Effective normal modes (blue arrows) at $T=20$ K and normal modes (red arrows) of H_2CO. Modes have increasing frequency from left to right and top to bottom.

the matrices of their Fourier transformed over the 32 molecules, prior to the construction of the effective normal modes.

Figure 3 displays the power spectra of the reconstructed effective normal modes in the rotating Eckart *frame*, on one hand, and the *coordinate system*, on the other hand. The HOH bending mode appears separated from the other modes with small overlaps. The two OH stretch modes are well separated from the other modes, but the overlap between these two is large. This is due to the important inhomogeneous broadening of the OH stretch vibrations in water, which is larger than the frequency gap between the symmetric and antisymmetric stretches. This also makes difficult the right distinction between symmetric and asymmetric stretches which should be attained with perfect statistics, but this is not the case for the small run (3 ps) used here. The precision on the average frequency of each band should be for this purpose smaller than the gap between the two modes, which is obviously not achieved here. However, it can clearly be seen from Fig. 4 that the lowest stretching mode has a definite symmetric character, while the highest frequency one has an antisymmetric character.

These three vibrational modes of one water molecule in liquid water are nearly independent of the choice of the Eckart framework or the coordinate system attached to it, while using the laboratory frame (see Fig. 4). In the laboratory frame, however, we also have access to information concerning translational and librational motions of the water molecule (see Fig. 3). We find three translational modes in the region between 50 and 400 cm^{-1} and three librational modes between 400 and 1000 cm^{-1}. One of the translational modes, translation along the HOH bisector, has a power spectra different from the other two, with a marked peak at 250 cm^{-1}, probably associated with hydrogen bonding.[45] The three librations are also not equivalent: the librational mode corresponding to a rotation of the water molecule around the axis perpendicular to its molecular plane is centered around 550 cm^{-1}, while the two other ones are centered around 750 cm^{-1}. In the laboratory frame (still using the coordinate system associated to the Eckart frame) we do have a complete picture of the individual motion of one water molecule in liquid water.

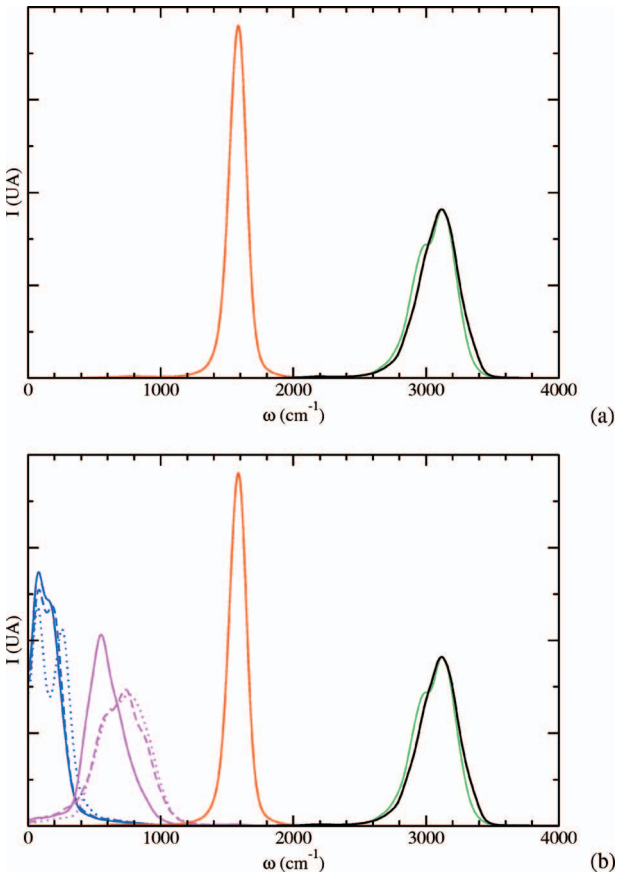

FIG. 3. (Color) Power spectra of the effective normal modes in the rotating Eckart *frame* (a) and in the *laboratory* frame using the coordinate system of the Eckart frame (b) (see text). In both frames, the solid red curve corresponds to the power spectrum of the water bending mode, while the green curve and the black solid curves correspond to the power spectra of the symmetric and asymmetric stretches, respectively. In (b), the blue curves represent the power spectra of water translation modes (solid: translation perpendicular to the molecular plane, dashed: translation along the HH vector, dotted: translation along the OHO bisectrix), while the pink curves represent the power spectra of the librational modes (solid: rotation in the molecular plane, dashed and dotted: rotation around the two OH axes).

D. Uracil in aqueous solution

As a last example, we have studied the effective normal modes of a more complex molecule, namely, a uracil molecule (see Fig. 5) in aqueous solution. The solvation of a uracil molecule in water and its infrared spectrum have been studied by DFT-based MD by Gaigeot and Sprik with good agreement with experiment. A detailed description and discussion of the hydrogen bonding network between uracil and

FIG. 4. (Color) Effective normal modes of a water molecule in liquid water (bend, symmetric and asymmetric stretches), in the Eckart frame (blue arrows), and in the coordinate system associated to the Eckart frame (red arrows).

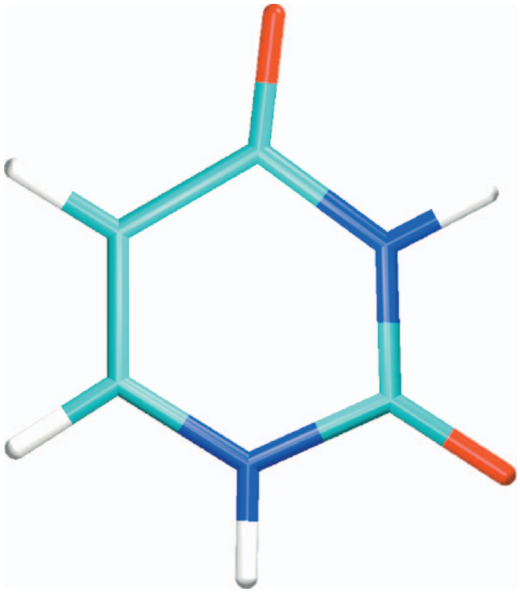

FIG. 5. (Color) A ball and stick representation of the uracil molecule. Hydrogen atoms are white, carbon cyan, nitrogen are blue, and oxygen atoms are in red.

the bulk solvent is presented in Ref. 7. Moreover, a thorough investigation of the IR spectrum of gas phase and liquid phase uracil is reported in Ref. 8 particularly in relation with uracil-water H bonds. IR band position shifts as well as band intensity variations in going from gas to liquid phase have been identified. However, the interpretation of the infrared spectrum extracted from MD turned out to be a highly non trivial task: we propose here to construct the effective normal modes for this system. The system consisted of one uracil molecule and 49 water molecules for which 7 ps of dynamics were generated with a time step $\delta t=0.12$ fs at $T=300$ K. Sampling was performed at each time step. The relatively short simulation time used in Ref. 8 was shown, however, to yield accurate band positions and intensities in the 1000–2000 cm^{-1} vibrational region relative to experiment: this favorable situation probably arises from the high frequencies of the modes of interest and the lack of large conformational motion in uracil.

Figure 6 shows the power spectra of the effective normal modes of the solvated uracil in the 1000–1700 cm^{-1} region. The effective normal modes in this region are displayed in Figs. 7 and 8. Each principal peak with a large amplitude can then be assigned to an effective normal mode, and most of them are well detached from the others with a small overlap. The effective normal mode analysis can help to get a more accurate assignment of the IR spectrum of uracil in aqueous solution (see Figs. 7 and 8). We find that the bands around 1600 cm^{-1} are made of three modes, mixing of the two C═O stretches and the C═C stretch, as proposed by Gaigeot and Sprik.[8] Around 1400 cm^{-1} we find mainly NH bending modes and at lower frequencies CH bendings with contributions from the NH bendings. However, the mode at 1166 cm^{-1} that was previously assigned to a C═C stretch here appears to be one N–C stretch.

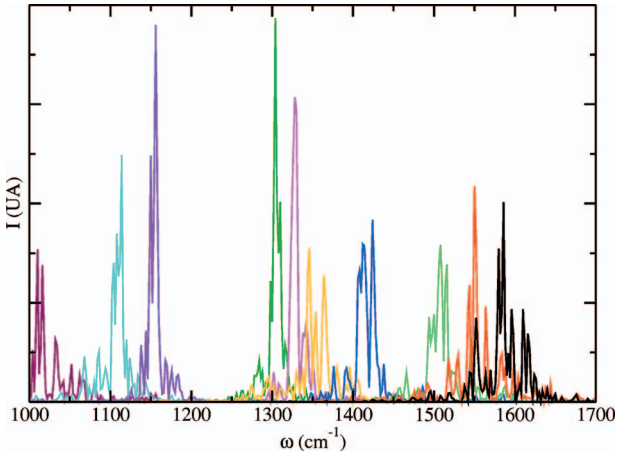

FIG. 6. (Color) Power spectra of the effective normal modes of one uracil molecule in aqueous solution between 1000 and 1700 cm^{-1}.

In the region of 1500–1600 cm^{-1}, the C═C and C═O stretches exhibit large shifts compared to their gas phase counterparts. In Ref. 8 hydrogen bonds were identified between the uracil oxygens and surrounding water molecules; these are probably responsible for the observed shifts. The same behavior has been described by Nonella *et al.*[10] for a *p*-benzoquinone in aqueous phase. The coupling between these modes will then depend a lot on the hydrogen bonding configuration. Here also we thus find a large inhomogeneous broadening with a substantial overlap between the power spectra of these three modes.

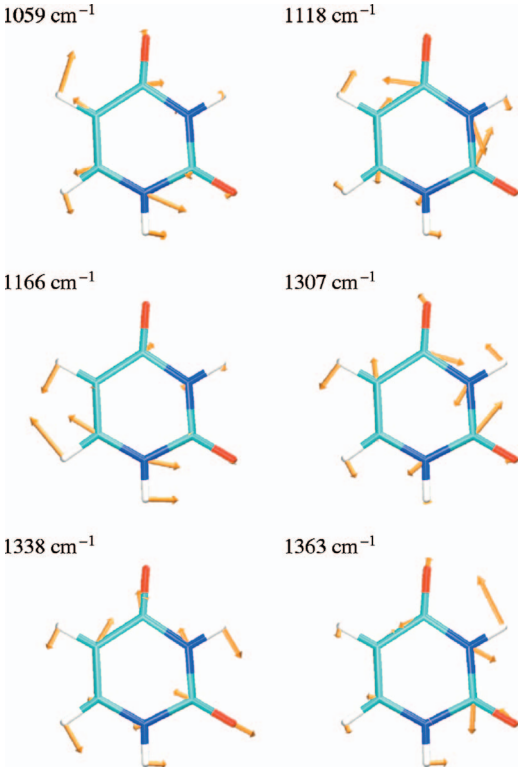

FIG. 7. (Color) Effective normal modes of one uracil molecule in aqueous solution between 1000 and 1400 cm^{-1}.

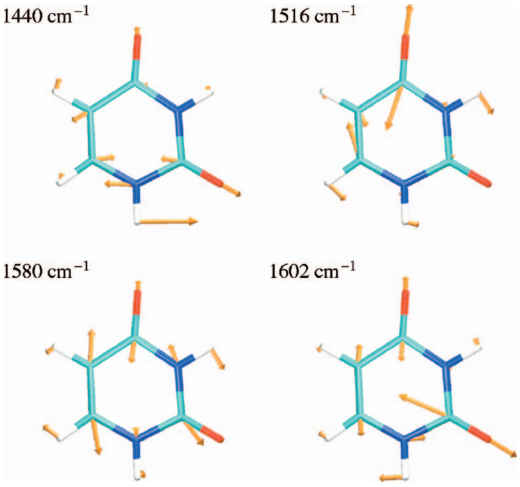

FIG. 8. (Color) Effective normal modes of one uracil molecule in aqueous solution between 1400 and 1700 cm^{-1}.

IV. CONCLUSION

We have presented a method for decomposing vibrational spectra in effective normal mode contributions, introducing a general definition for these through maximum localization of the power spectra in frequency space. There is then a freedom left as of the function to characterize the spread of a power spectrum and to be minimized. Here we have limited ourselves to the minimization of the quantity $\langle\omega^{2n}\rangle-\langle\omega^{n}\rangle^{2}$ and we focused our attention on the $n=2$ and $n=-2$ cases. For the two cases, the solution of the minimization procedure can be found then through a generalized eigenvalue problem, where the eigenvalues turn out to be typical frequencies of the effective normal mode motions. For $n=-2$ the present method shares strong analogy with covariant matrices or PMA methods previously introduced in the literature,[27,28,33,34] with the additional feature of accounting for finite statistics effects. $n=2$ leads to a new route for determining vibrational modes and frequencies through a strict generalization of the normal mode definition[37] to finite temperature. This approach is applicable also when the simulated trajectories from which effective normal modes are extracted do not satisfy strict equipartition.

For both $n=-2$ and $n=2$, accounting for finite statistics is achieved by a proper choice of normalization of the power spectra. This normalization procedure leads to a few advantages. First it yields the usual definition of normal modes as unitary transforms of mass weighted coordinates for a system at equilibrium, in the canonical or microcanonical ensembles. It can be viewed as an extension of that prescription to finite trajectories. We showed that it can be strictly derived from a force-fitting procedure, where the exact forces are approximated by their best harmonic fit, in a least-squares sense. Consequently, we argued theoretically, and verified numerically, that the typical mode frequencies obtained this way have little dependence on whether equipartition is well satisfied or not by the simulation. This is reminiscent of the generalized virial approach introduced by Schmitz and Tavan.[33,34]

We have studied three examples and have extracted, using DFT-based MD trajectories, the effective normal modes of a formaldehyde molecule in gas phase and of a water molecule and a uracil molecule in liquid water. We have limited our practical applications to the $n=2$ case since (i) we believe that, in analogy with the usual normal mode analysis, it provides a much more natural definition of finite temperature effective normal modes from an averaged Hessian, and (ii) in contrast to PMA, it can be applied to diffusive modes as illustrated for water translations and librations, for which the power spectra do not go to zero at zero frequency [see Fig. 3(b)]. As we could check in preliminary tests this feature is important too when studying the vibrational signature of rotating groups, e.g., –CH_3 groups. In that case, the covariance matrix description becomes pathological.

The present approach is not limited to gas or liquid phase but can be straightforwardly applied to solid phase systems, either amorphous or crystalline. In the case of crystals, MD simulation of a supercell can be shown to lead through translational invariance to effective normal modes having a well-defined wave vector in the Brillouin zone of the crystal. It should then be possible to reconstruct dispersion curves from MD simulations at finite temperature, avoiding the frozen phonon approximation for anharmonic effects. Work in this direction is underway.

The new method that we propose for decomposing vibrational spectra from force-force and momentum-momentum correlation functions has a quite general applicability, and it presents a very small computational overhead, basically equivalent to that involved in principal mode analysis. The examples presented here illustrated the possibility to extract with this new method vibrational modes from *ab initio* molecular dynamics trajectory without any extra information but the trajectory itself. However, the present method should be most useful when the vibrational modes differ significantly from the zero temperature normal modes in gas phase. Future extensions also involve the use of internal coordinates rather than Cartesian coordinates. This, in particular, avoids the definition of a molecular frame and should be better adapted to large and floppy (bio)molecules.

APPENDIX A: MAXIMIZATION OF $\Omega'^{(n)}$

We show here that the solution $\mathbf{Y}^0$ to the generalized eigenvalue problem,

$$K_{p\,ij}^{(n)}Y_{jk}^{0}=\lambda_{k}^{(n)}K_{p\,ij}^{(0)}Y_{jk}^{0}, \tag{A1a}$$

$$\mathbf{K}_{p}^{(n)}\mathbf{Y}^{0}=\mathbf{K}_{p}^{(0)}\mathbf{Y}^{0}\Lambda, \tag{A1b}$$

under the constraint of Eq. (26), also maximizes $\Omega'^{(n)}$ (Λ is a diagonal matrix with $\lambda_k^{(n)}$, where $k=1,\ldots,3N$ on the diagonal). To this end, we will study the effect of an infinitesimal perturbation of $\mathbf{Y}^0$ by considering the transformation matrix

$$\mathbf{Y}=\mathbf{Y}^{0}e^{\epsilon A}=\mathbf{Y}^{0}+\epsilon\mathbf{Y}^{0}\mathbf{A}+\frac{\epsilon^{2}}{2}\mathbf{Y}^{0}\mathbf{A}^{2}+\cdots, \tag{A2}$$

where $\mathbf{A}$ is an antisymmetric matrix so that $\mathbf{Y}$ still satisfies constraint (26) ($e^{\epsilon A}$ is a unitary matrix). Writing $\Omega'^{(n)}$ to first order in ϵ,

$$\frac{\partial \Omega'^{(n)}}{\partial \epsilon} = 2\sum_k (\mathbf{Y}^{0^T}\mathbf{K}_p^{(n)}\mathbf{Y}^0)_{kk}(2\mathbf{A}\mathbf{Y}^{0^T}\mathbf{K}_p^{(n)}\mathbf{Y}^0)_{kk} \tag{A3a}$$

$$= 4\sum_k \lambda_k^{(n)}(\mathbf{A}\mathbf{Y}^{0^T}\mathbf{K}_p^{(n)}\mathbf{Y}^0)_{kk}. \tag{A3b}$$

However, $\mathbf{Y}^{0^T}\mathbf{K}_p^{(n)}\mathbf{Y}^0 = \mathbf{Y}^{0^T}\mathbf{K}_p^{(0)}\mathbf{Y}^0\Lambda = \Lambda$, so that $(2\mathbf{A}\mathbf{Y}^{0^T}\mathbf{K}_p^{(n)}\mathbf{Y}^0)_{kk} = 2A_{kk}\lambda_k^{(n)} = 0$ since $\mathbf{A}$ is antisymmetric. Thus $\mathbf{Y}^0$ is indeed an extremum of $\Omega'^{(n)}$.

At second order in ϵ, we have, using the preceding result,

$$\frac{1}{2}\frac{\partial^2 \Omega'^{(n)}}{\partial \epsilon^2} = 2\sum_k \lambda_k^{(n)}\{-(\mathbf{A}\mathbf{Y}^{0^T}\mathbf{K}_p^{(n)}\mathbf{Y}^0\mathbf{A})_{kk} + (\mathbf{A}\mathbf{A}\mathbf{Y}^{0^T}\mathbf{K}_p^{(n)}\mathbf{Y}^0)_{kk}\} \tag{A4a}$$

$$= -2\sum_{kl} \lambda_k^{(n)}A_{kl}\lambda_l^{(n)}A_{lk} + 2\sum_{kl} \lambda_k^{(n)^2}A_{kl}A_{lk} \tag{A4b}$$

$$= -2\sum_{kl} A_{kl}A_{lk}\lambda_k^{(n)}\lambda_l^{(n)} + A_{kl}A_{lk}\left(\frac{\lambda_k^{(n)^2}}{2} + \frac{\lambda_l^{(n)^2}}{2}\right) \tag{A4c}$$

$$= \sum_{kl} A_{kl}A_{lk}(\lambda_k^{(n)} - \lambda_l^{(n)})^2 \tag{A4d}$$

$$= -\sum_{kl} A_{kl}^2(\lambda_k^{(n)} - \lambda_l^{(n)})^2 \leqslant 0, \tag{A4e}$$

and $\mathbf{Y}^0$ is found to actually maximize $\Omega'^{(n)}$.

APPENDIX B: CALCULATION OF $\mathbf{K}_x^{(-2)}$

We want in this appendix to calculate the matrix elements of $\mathbf{K}_x^{(-2)}$,

$$(\mathbf{K}_x^{(-2)})_{ij} = \frac{\beta}{2\pi}\mathcal{P}\int_{-\infty}^{+\infty} d\omega\omega^{-2}P_{ij}^{\dot{x}}(\omega)$$

$$= \frac{\beta}{2\pi}\mathcal{P}\int_{-\infty}^{+\infty} d\omega\omega^{-2}\mathrm{TF}[\langle \dot{x}_i(0)\dot{x}_j(t)\rangle](\omega), \tag{B1}$$

where $\mathcal{P}$ denotes a principal part, that is,

$$(\mathbf{K}_x^{(-2)})_{ij} = \frac{\beta}{2\pi}\lim_{\epsilon\to\infty}\int_{\epsilon}^{+\infty} d\omega\omega^{-2}\mathrm{TF}[\langle \dot{x}_i(0)\dot{x}_j(t)\rangle](\omega)$$

$$+ \int_{-\infty}^{-\epsilon} d\omega\omega^{-2}\mathrm{TF}[\langle \dot{x}_i(0)\dot{x}_j(t)\rangle](\omega). \tag{B2}$$

We assume here that

$$\int_{-\infty}^{\infty} \langle \dot{x}_i(0)\dot{x}_j(t)\rangle dt = 0, \tag{B3}$$

which means that there should be no diffusive modes in principle in the system under consideration, and we further assume that $\langle \dot{x}_i(0)\dot{x}_j(t)\rangle \to 0$ as $t\to\infty$ sufficiently fast so that $(\mathbf{K}_x^{(-2)})_{ij}$ is defined.

Defining $\delta x_i = x_i - \langle x_i\rangle$ the atomic displacements with respect to the average atomic position, we have

$$\frac{d^2}{dt^2}\langle \delta x_i(0)\delta x_j(t)\rangle = -\langle \dot{x}_i(0)\dot{x}_j(t)\rangle, \tag{B4}$$

which can be expressed after the Fourier transformation as

$$\omega^2\mathrm{TF}[\langle \delta x_i(0)\delta x_j(t)\rangle](\omega) = \mathrm{TF}[\langle \dot{x}_i(0)\dot{x}_j(t)\rangle](\omega). \tag{B5}$$

For all $\omega \neq 0$ we then have

$$\mathrm{TF}[\langle \delta x_i(0)\delta x_j(t)\rangle](\omega) = \frac{1}{\omega^2}\mathrm{TF}[\langle \dot{x}_i(0)\dot{x}_j(t)\rangle](\omega), \tag{B6}$$

and thus

$$(\mathbf{K}_x^{(-2)})_{ij} = \frac{\beta}{2\pi}\lim_{\epsilon\to 0}\int_{\epsilon}^{+\infty} d\omega\mathrm{TF}[\langle \delta x_i(0)\delta x_j(t)\rangle](\omega)$$

$$+ \int_{-\infty}^{-\epsilon} d\omega\mathrm{TF}[\langle \delta x_i(0)\delta x_j(t)\rangle](\omega). \tag{B7}$$

From $\langle \delta x_i(0)\delta x_j(t)\rangle \to 0$ as $t\to\infty$ and assuming that the decorrelation is again fast enough, $\lim_{\omega\to 0}\mathrm{TF}[\langle \delta x_i(0)\delta x_j(t)\rangle](\omega) = \int dt\langle \delta x_i(0)\delta x_j(t)\rangle$ is defined and the function $\mathrm{TF}[\langle \delta x_i(0)\delta x_j(t)\rangle](\omega)$ is continuous in $\omega = 0$ so that we can take the limit $\epsilon\to 0$ in the previous expression and finally obtain

$$(\mathbf{K}_x^{(-2)})_{ij} = \frac{\beta}{2\pi}\int_{-\infty}^{+\infty} d\omega\mathrm{TF}[\langle \delta x_i(0)\delta x_j(t)\rangle](\omega) \tag{B8}$$

$$= \langle \delta x_i(0)\delta x_j(t)\rangle|_{t=0} = \langle \delta x_i\delta x_j\rangle. \tag{B9}$$

APPENDIX C: HARMONIC POTENTIAL FORCE FITTING

We want to fit the forces F_i on the atoms as a linear combination of the displacements

$$F_i \approx -k_{i1}\delta x_1 - \cdots - k_{i,3N}\delta x_{3N} = -k_{ij}\delta x_j. \tag{C1}$$

To this purpose the coefficients k_{ij} are obtained by a least-squares fit, minimizing

$$\chi = \sum_i \langle (F_i + k_{i1}\delta x_1 + \cdots + k_{i,3N}\delta x_{3N})^2\rangle. \tag{C2}$$

The result of this least-squares fit can be explicitly constructed from

$$\frac{\partial \chi}{\partial k_{ij}} = 2\langle \delta x_j(k_{ik}\delta x_k + F_i)\ = 2\langle F_i\delta x_j\rangle + 2k_{ik}\langle \delta x_k\delta x_j\rangle = 0 \tag{C3}$$

at the minimum. Rewriting the last equality in a matrix form, we have

$$\langle \mathbf{F}\delta\mathbf{x}^T\rangle + k\langle \delta\mathbf{x}\delta\mathbf{x}^T\rangle = 0, \tag{C4}$$

that is,

$$k = -\langle \mathbf{F}\delta\mathbf{x}^T\rangle \cdot (\langle \delta\mathbf{x}\delta\mathbf{x}^T\rangle)^{-1}. \tag{C5}$$

[1] R. Car and M. Parrinello, Phys. Rev. Lett. **55**, 2471 (1985).
[2] P. L. Silvestrelli, M. Bernasconi, and M. Parrinello, Chem. Phys. Lett. **277**, 478 (1997).
[3] V. Dubois, P. Umari, and A. Pasquarello, Chem. Phys. Lett. **390**, 193 (2004).
[4] J.-W. Handgraaf, E. J. Meijer, and M.-P. Gaigeot, J. Chem. Phys. **121**, 10111 (2004).
[5] D. E. Bikiel, F. D. Salvo, M. C. G. Lebrero, F. Doctorovich, and D. A. Estrin, Inorg. Chem. **44**, 5286 (2005).
[6] M. Gaigeot, R. Vuilleumier, M. Sprik, and D. Borgis, J. Chem. Theory Comput. **1**, 772 (2005).
[7] M.-P. Gaigeot and M. Sprik, J. Phys. Chem. B **108**, 7458 (2004).
[8] M.-P. Gaigeot and M. Sprik, J. Phys. Chem. B **107**, 10344 (2003).
[9] R. Iftimie and M. E. Tuckerman, J. Chem. Phys. **122**, 214508 (2005).
[10] M. Nonella, G. Mathias, and P. Tavan, J. Phys. Chem. A **107**, 8638 (2003).
[11] A. Putrino, D. Sebastiani, and M. Parrinello, J. Chem. Phys. **113**, 7102 (2000).
[12] A. Putrino and M. Parrinello, Phys. Rev. Lett. **88**, 176401 (2002).
[13] R. Resta, Phys. Rev. Lett. **80**, 1800 (1998).
[14] R. Kubo, M. Toda, and N. Hashitsume, *Statistical Physics*, 2nd ed. (Springer, Berlin, 1991), Vol. II.
[15] J. M. Bowman, X. Zhang, and A. Brown, J. Chem. Phys. **119**, 646 (2003).
[16] M. Kaledin, A. Brown, A. Kaledin, and J. M. Bowman, J. Chem. Phys. **121**, 5646 (2004).
[17] J. Kohanoff, Comput. Mater. Sci. **2**, 221 (1994).
[18] G. Onida, W. Andreoni, J. Kohanoff, and M. Parrinello, Chem. Phys. Lett. **219**, 1 (1994).
[19] M. C. G. Lebrero, L. L. Perissinotti, and D. A. Estrin, J. Phys. Chem. A **109**, 9598 (2005).
[20] R. M. Stratt, Acc. Chem. Res. **28**, 201 (1995).
[21] M. Buchner, B. Ladanyi, and R. M. Stratt, J. Chem. Phys. **97**, 8522 (1992).
[22] M. Cho, G. R. Fleming, S. Saito, I. Ohmine, and R. M. Stratt, J. Chem. Phys. **100**, 6672 (1994).
[23] R. E. Larsen and R. M. Stratt, J. Chem. Phys. **110**, 1036 (1999).
[24] M. Nonella, G. Mathias, M. Eichinger, and P. Tavan, J. Phys. Chem. B **107**, 316 (2003).
[25] L. Pejov, D. Spangberg, and K. Hermansson, J. Phys. Chem. A **109**, 5144 (2005).
[26] R. M. Levy, O. de la Luz Rojas, and R. A. Friesner, J. Phys. Chem. **88**, 4233 (1984).
[27] R. A. Wheeler, H. Dong, and S. E. Boesch, ChemPhysChem **4**, 382 (2003).
[28] R. A. Wheeler and H. Dong, ChemPhysChem **4**, 1227 (2003).
[29] B. R. Brooks, D. Janezic, and M. Karplus, J. Comput. Chem. **16**, 1522 (1995).
[30] A. Amadei, A. B. M. Linssen, and H. J. C. Berendsen, Proteins: Struct., Funct., Genet. **17**, 412 (1993).
[31] F. Tama, F. X. Gadea, O. Marques, and Y.-H. Sanejouand, Proteins: Struct., Funct., Genet. **41**, 1 (2000).
[32] F. Tama and Y.-H. Sanejouand, Protein Eng. **14**, 1 (2001).
[33] M. Schmitz and P. Tavan, J. Chem. Phys. **121**, 12247 (2004).
[34] M. Schmitz and P. Tavan, J. Chem. Phys. **121**, 12233 (2004).
[35] A. Strachan, J. Chem. Phys. **120**, 1 (2004).
[36] D. J. Evans, O. G. Jepps, and G. Ayton, Phys. Rev. E **62**, 4757 (2000).
[37] E. B. Wilson, J. Decius, and P. C. Cross, *Molecular Vibrations* (Dover, New York, 1955).
[38] B. Butler, G. Ayton, O. G. Jepps, and D. J. Evans, J. Chem. Phys. **109**, 6519 (1998).
[39] C. Eckart, Phys. Rev. **47**, 552 (1935).
[40] A. D. Becke, Phys. Rev. A **38**, 3098 (1988).
[41] C. Lee, W. Yang, and R. G. Parr, Phys. Rev. B **37**, 785 (1988).
[42] N. Troullier and J. L. Martins, Phys. Rev. B **43**, 1993 (1991).
[43] L. Kleinman and D. M. Bylander, Phys. Rev. Lett. **48**, 1425 (1982).
[44] CPMD, IBM Corp., 1990–2001/MPI für Festkörperforschung Stuttgart, 1997–2004.
[45] M. Sharma, R. Resta, and R. Car, Phys. Rev. Lett. **95**, 187401 (2005).